

EFFECT ON UNIFORM AND NON UNIFORM TEMPERATURE GRADIENTS ON BENARD-MARANGONI CONVECTION IN A SUPERPOSED FLUID AND POROUS LAYER IN THE PRESENCE OF HEAT SOURCE

VANISHREE R K¹ , SUMITHRA R² and MANJUNATHA N^{3,*}

¹Department of Mathematics, Maharani's Science College for Women,
Maharani Cluster University, Bengaluru, Karnataka, India;

Email: vanirkmscw@gmail.com

² Department of UG, PG Studies & Research in Mathematics, Government
Science College Autonomous, Bengaluru, Karnataka, India;

Email: sumitra_diya@yahoo.com

^{3,*} School of Applied Sciences, REVA University, Bengaluru, Karnataka,
India;

Email: manjunatha.n@reva.edu.in

ABSTRACT. *Effect of uniform and non uniform temperature gradients on Bènard-Marangoni convection in a superposed fluid and porous (composite) layer in the presence of constant heat source (sink) is studied under microgravity condition. The Eigen value, thermal Marangoni number, of the problem is obtained in the closed form for free-rigid velocity boundary combinations with adiabatic and isothermal boundary conditions at the boundaries. The influence of various parameters against depth ratio is discussed. It is observed that the effect of heat source (sink) is predominant in porous layer. The parameters influence on advancing or delaying convection is analyzed.*

AMS Subject Classification: 80-XX, 80Axx, 80A20.

Keywords: Non uniform temperature gradients, Bènard-Marangoni convection, composite layer, heat source (sink).

1. INTRODUCTION

Marangoni convection which is induced by a surface tension gradient on the interface is an important phenomenon under microgravity conditions. Convection in a composite layer system consisting of two layers with a fluid saturated porous layer underneath the fluid layer has many applications in engineering and industrial problems such as flow of water under earth's surface, drying silicon wafers after a wet processing step during the manufacture of integrated circuits, self-assembling of nanoparticles into ordered arrays to grow ordered nanotubes, crystal growth and so on. Most of these processes involve controlling of convection. This can be achieved by maintaining non-uniform temperature gradients across the composite layer. Such a temperature gradient can be generated by:

- (i) an appropriate type of heating or cooling at boundaries,
- (ii) an appropriate internal heat generation
- (iii) injection/suction (through-flow) of fluid at the boundaries.

Marangoni convection in composite layers is understood and well documented (see Nield [1], McKay [2], Taslim and Narusawa [3], Chen [4]. A review is given in detail by Nield and Bejan [5] with relevant literature including Straughan ([6], [7]), Carr [8], Chang ([9], [10], [11]), Shivakumara *et al.* [12]).

Recent works on Bènard-Marangoni convection in composite layers have thrown light on the mechanism. The condition for the onset of Marangoni convection in the presence of temperature gradients in a two-layer system comprising of a fluid saturated anisotropic porous beneath a fluid layer was obtained by Shivakumara *et al.* [13], later Shivakumara *et al.* [14] extended the study of Shivakumara *et al.* [13] to include the effects of internal heating. Marangoni convection driven by a power law temperature gradient was considered by Zheng *et al.* [15]. Sumithra and Manjunatha [16] studied analytically the Marangoni convection in a composite layer in the presence of magnetic field. Sumithra [17] analyzed the double diffusive magneto-Marangoni convection in a composite layer. Tatiana [18] used different methods for modulation of Marangoni convection and Marangoni induced interface deformation in non-isotherm liquid films. Marangoni convection in a voltaic liquid film subject to a horizontal temperature gradient confined in a rectangular cavity was studied by Li and Yoda [19]. Sankaran and Yarin [20] analysed the evaporation driven thermocapillary Marangoni convection in liquid layers of different depths. Influence of vertical magnetic field on the onset of Rayleigh-Bènard-Marangoni convection in a composite layer with deformable free surface was investigated by Anand and Gangadharaiiah [21]. Manjunatha and Sumithra [22] considered the effect of non-uniform temperature gradients on double diffusive Marangoni convection in a two layer system.

Internal heat source (sink) can also be used as an effective parameter to control convection. Internal heat source (sink) may arise due to heat released during chemical reactions in the fluid, radioactive decay, Ohmic heating by current in conductive liquid, produced by radiation from external medium there by helping in advancing or delaying convection. The influence of heat source sink in convection phenomenon is studied exhaustively (see Vanishree [23], Siddheshwar and Vanishree [24] and the references therein).

In the present paper an attempt is made to study the effect of non-uniform temperature gradients on Bènard-Marangoni convection in a superposed fluid and porous layer in the presence of a constant heat source (sink) of same strength in both the layers.

2. FORMULATION OF THE PROBLEM

Consider a horizontal single component, fluid saturated isotropic densely packed porous layer of thickness d_m underlying a single component fluid layer of thickness d with heat sources Q_m and Q respectively. The lower surface of the porous layer rigid and the upper surface of the fluid layer is free with surface tension effects depending on temperature. A Cartesian coordinate system is chosen with the origin at the interface between porous and fluid layers and the z-axis, vertically upwards. The basic equations governing such a system are,

$$\nabla \cdot \vec{q} = 0 \tag{1}$$

$$\rho_0 \left[\frac{\partial \vec{q}}{\partial t} + (\vec{q} \cdot \nabla) \vec{q} \right] = -\nabla P + \mu \nabla^2 \vec{q} \tag{2}$$

$$\frac{\partial T}{\partial t} + (\vec{q} \cdot \nabla) T = \kappa \nabla^2 T + Q \tag{3}$$

$$\nabla_m \cdot \vec{q}_m = 0 \tag{4}$$

$$\rho_0 \left[\frac{1}{\varepsilon} \frac{\partial \vec{q}_m}{\partial t} + \frac{1}{\varepsilon^2} (\vec{q}_m \cdot \nabla_m) \vec{q}_m \right] = -\nabla_m P_m - \frac{\mu}{K} \vec{q}_m \tag{5}$$

$$A \frac{\partial T_m}{\partial t} + (\vec{q}_m \cdot \nabla_m) T_m = \kappa_m \nabla_m^2 T_m + Q_m \tag{6}$$

where \vec{q} is the velocity vector, ρ_0 is the fluid density, t is the time, μ is the fluid viscosity, P is the pressure, T is the temperature, κ is the thermal diffusivity of the fluid, Q is the constant heat source, ε is the porosity, K is the permeability of the porous medium, $A = \frac{(\rho_0 C_p)_m}{(\rho_0 C_p)_f}$ is the ratio of heat capacities, C_p is the specific heat, κ_m is the thermal diffusivity of the porous layer, Q_m is the constant heat source for porous layer and the subscripts 'm' refer to the porous layer and 'f' refer to the fluid layer.

The basic state of fluid and porous layer is quiescent, have the following solutions

$$\vec{q} = \vec{q}_b = 0, P = P_b(z), T = T_b(z) \tag{7}$$

$$\vec{q}_m = \vec{q}_{mb}, P_m = P_{mb}(z_m), T_m = T_{mb}(z_m) \tag{8}$$

$$T_b(z) = \frac{-Qz(z-d)}{2\kappa} + \frac{(T_u - T_0)h(z)}{d} + T_0 \quad 0 \leq z \leq d \tag{9}$$

$$T_{mb}(z_m) = \frac{-Q_m z_m(z_m + d_m)}{2\kappa_m} + \frac{(T_0 - T_l)h_m(z_m)}{d_m} + T_0 \quad -d_m \leq z_m \leq 0 \tag{10}$$

where $T_0 = \frac{\kappa d_m T_u + \kappa_m d T_l}{\kappa d_m + \kappa_m d} + \frac{d d_m (Q_m d_m + Q d)}{2(\kappa d_m + \kappa_m d)}$ is the interface temperature and $h(z)$ and $h_m(z_m)$ are temperature gradients in fluid and porous layer respectively and subscript 'b' denote the basic state.

To study the stability of the basic state, we superimpose infinitesimally small perturbations on the basic state for fluid and porous layer respectively

in the form

$$\vec{q} = \vec{q}_b + \vec{q}', P = P_b + P', T = T_b(z) + \theta, \tag{11}$$

$$\vec{q}_m = \vec{q}_{mb} + \vec{q}'_m, P_m = P_{mb} + P'_m, T_m = T_{mb}(z_m) + \theta_m \tag{12}$$

where the prime indicates the perturbations. Introducing (11) and (12) in (1) - (6), operating curl twice and eliminate the pressure term from equations (2) and (5), the resulting equations then non dimensionalized.

The dimensionless equations are then subjected to normal mode analysis procedure in the form

$$\begin{bmatrix} W \\ \theta \end{bmatrix} = \begin{bmatrix} W(z) \\ \theta(z) \end{bmatrix} f(x, y)e^{nt} \tag{13}$$

$$\begin{bmatrix} W_m \\ \theta_m \end{bmatrix} = \begin{bmatrix} W_m(z_m) \\ \theta_m(z_m) \end{bmatrix} f_m(x_m, y_m)e^{n_mt} \tag{14}$$

with $\nabla_2^2 f + a^2 f = 0$ and $\nabla_{2m}^2 f_m + a_m^2 f_m = 0$, where a and a_m are the nondimensional horizontal wave numbers, n and n_m are the frequencies, $W(z)$ and $W_m(z_m)$ are the dimensionless vertical velocities in fluid and porous layer respectively and obtain the following equations in $0 \leq z \leq 1$

$$(D^2 - a^2 + \frac{n}{Pr})(D^2 - a^2)W(z) = 0 \tag{15}$$

$$(D^2 - a^2 + n)\theta(z) + [h(z) + R_I^*(2z - 1)]W(z) = 0 \tag{16}$$

in $-1 \leq z_m \leq 0$

$$(D_m^2 - a_m^2)W_m(z_m) = 0 \tag{17}$$

$$(D_m^2 - a_m^2 + An_m)\theta_m(z_m) + [h_m(z_m) + R_{Im}^*(2z_m + 1)]W_m(z_m) = 0 \tag{18}$$

where Pr is the prandtl number, $R_I^* = \frac{R_I}{2(T_0 - T_u)}$, $R_{Im}^* = \frac{R_{Im}}{2(T_l - T_0)}$, R_I is the internal Rayleigh number for fluid layer and R_{Im} is the internal Rayleigh number for porous layer.

Assume that the present problem is satisfies the principle of exchange of stability, so putting $n = n_m = 0$. We get, in $0 \leq z \leq 1$

$$(D^2 - a^2)^2 W(z) = 0 \tag{19}$$

$$(D^2 - a^2)\theta(z) + [h(z) + R_I^*(2z - 1)]W(z) = 0 \tag{20}$$

in $-1 \leq z_m \leq 0$

$$(D_m^2 - a_m^2)W_m(z_m) = 0 \tag{21}$$

$$(D_m^2 - a_m^2)\theta_m(z_m) + [h_m(z_m) + R_{Im}^*(2z_m + 1)]W_m(z_m) = 0 \tag{22}$$

3. BOUNDARY CONDITIONS

The boundary conditions are nondimensionalized and then subjected to normal mode expansion and are

$$\begin{aligned}
 D^2W(1) + Ma^2\theta(1) &= 0, \\
 W(1) = 0, W_m(-1) = 0, \widehat{T}W(0) &= W_m(0), \\
 \widehat{T}\widehat{d}^2(D^2 + a^2)W(0) &= (D_m^2 + a_m^2)W_m(0), \\
 \widehat{T}\widehat{d}^3(D^3W(0) - 3a^2DW(0)) &= -\beta D_mW_m(0), \\
 D\theta(1) = 0, \theta(0) = \widehat{T}\theta_m(0), \\
 D\theta(0) = D_m\theta_m(0), \theta_m(-1) &= 0
 \end{aligned} \tag{23}$$

where

$\widehat{T} = \frac{T_l - T_0}{T_0 - T_u}$ is the thermal ratio, $M = -\frac{\partial\sigma_t}{\partial T} \frac{(T_0 - T_u)d}{\mu\kappa}$ is the thermal Marangoni number, $\beta = \frac{d_m^2}{K}$ is the porous parameter and $\widehat{d} = \frac{d_m}{d}$ is the depth ratio.

4. METHOD OF SOLUTION

The solutions $W(z)$ and $W_m(z_m)$ are obtained by solving (19) and (21) using the velocity boundary conditions of (23)

$$\begin{aligned}
 W(z) &= A_1[\cosh az + a_1 \sinh az + a_2 z \cosh az + a_3 z \sinh az] \tag{24} \\
 W_m(z_m) &= A_1[a_4 \cosh a_m z_m + a_5 \sinh a_m z_m] \tag{25}
 \end{aligned}$$

where

$$\begin{aligned}
 a_1 &= \frac{\beta a_m \coth a_m}{2a^3 \widehat{d}}, a_2 = -1 - (a_1 + a_3) \tanh a, a_3 = \frac{a_m^2 - a^2 \widehat{d}^2}{a \widehat{d}^2}, \\
 a_4 &= \widehat{T}, a_5 = \widehat{T} \coth a_m
 \end{aligned}$$

4.1. Linear temperature profile.

Here taking

$$h(z) = 1 \quad \text{and} \quad h_m(z_m) = 1 \tag{26}$$

Substituting equation (26) into (20) and (22), the temperature distributions $\theta(z)$ and $\theta_m(z_m)$ are obtained using the temperature boundary conditions, as follows

$$\theta(z) = A_1[c_1 \cosh az + c_2 \sinh az + g_1(z)] \tag{27}$$

$$\theta_m(z_m) = A_1[c_3 \cosh a_m z_m + c_4 \sinh a_m z_m + g_{1m}(z_m)] \tag{28}$$

where

$$\begin{aligned}
 g_1(z) &= A_1[\Delta_1 - \Delta_2 + \Delta_3 - \Delta_4], g_{1m}(z_m) = A_1[\Delta_5 - \Delta_6] \\
 \Delta_1 &= \frac{(2E_1 z + E_2 z^2)}{4a} (a_1 \cosh az + \sinh az)
 \end{aligned}$$

$$\begin{aligned} \Delta_2 &= \frac{E_2 z}{4a^2} (\cosh az + a_1 \sinh az) \\ \Delta_3 &= \frac{(6a^2 z^2 E_1 + 4a^2 z^3 E_2 + 6E_2 z)}{24a^3} (a_3 \cosh az + a_2 \sinh az) \\ \Delta_4 &= \frac{(E_1 z + E_2 z^2)}{4a^2} (a_2 \cosh az + a_3 \sinh az) \\ \Delta_5 &= \frac{(2E_{1m} z_m + E_{2m} z_m^2)}{4a_m} (a_5 \cosh a_m z_m + a_4 \sinh a_m z_m) \\ \Delta_6 &= \frac{E_{2m} z_m}{4a_m^2} (a_4 \cosh a_m z_m + a_5 \sinh a_m z_m) \\ E_1 &= R_I^* - 1, E_2 = -2R_I^*, E_{1m} = -(R_{Im}^* + 1), E_{2m} = -2R_{Im}^* \\ c_1 &= c_3 \hat{T}, c_2 = \frac{1}{a} (c_4 a_m + \delta_3 - \delta_2), \\ c_3 &= \frac{\delta_6}{\delta_7}, c_4 = \frac{\delta_8}{\delta_9}, \delta_1 = -A_1 [\Delta_7 + \Delta_8 + \Delta_9 + \Delta_{10}] \\ \Delta_7 &= \frac{(2a^2 E_1 + E_2 (a^2 - 1))}{4a^2} (\cosh a + a_1 \sinh a) \\ \Delta_8 &= \frac{E_2 + 2E_1}{4a} (a_1 \cosh a + \sinh a) \\ \Delta_9 &= \frac{(3a^2 - 3)E_1 + (2a^2 - 3)E_2}{12a^2} (a_2 \cosh a + a_3 \sinh a) \\ \Delta_{10} &= \frac{(a^2 E_1 + E_2 (a^2 + 1))}{4a^3} (a_3 \cosh a + a_2 \sinh a) \\ \delta_2 &= A_1 \left[\frac{(2a^2 a_1 - a a_2) E_1 + (a_3 - a) E_2}{4a^3} \right] \\ \delta_3 &= A_1 \left[\frac{2E_{1m} a_5}{4a_m} - \frac{a_4 E_{2m}}{4a_m^2} \right] \\ \delta_4 &= -A_1 [\Delta_{11} + \Delta_{12}] \\ \Delta_{11} &= \left[\frac{E_{2m} - 2E_{1m}}{4a_m} \right] (a_5 \cosh a_m - a_4 \sinh a_m) \\ \Delta_{12} &= \left[\frac{E_{2m}}{4a_m^2} \right] (a_4 \cosh a_m - a_5 \sinh a_m) \\ \delta_5 &= \delta_1 - (\delta_3 - \delta_2) \cosh a, \delta_6 = \delta_4 a_m \cosh a + \delta_5 \sinh a_m \\ \delta_7 &= a_m \cosh a_m \cosh a + a \hat{T} \sinh a \sinh a_m \\ \delta_8 &= \delta_4 a \hat{T} \sinh a - \delta_5 \cosh a_m \\ \delta_9 &= -a \sinh a_m \hat{T} \sinh a - a_m \cosh a \cosh a_m \end{aligned}$$

From the boundary condition (23)¹, the thermal Marangoni number for the linear temperature profile is as follows

$$M_1 = \frac{-\Lambda_1}{a^2 (c_1 \cosh a + c_2 \sinh a + \Lambda_2 + \Lambda_3)} \tag{29}$$

where

$$\begin{aligned} \Lambda_1 &= \Delta_{13} + \Delta_{14} \\ \Delta_{13} &= a^2 (\cosh a + a_1 \sinh a) + a_2 (a^2 \cosh a + 2a \sinh a) \\ \Delta_{14} &= a_3 (a^2 \sinh a + 2a \cosh a) \\ \Lambda_2 &= \left(\frac{E_2 + 2E_1}{4a} \right) (a_1 \cosh a + \sinh a) - \frac{E_2}{4a^2} (\cosh a + a_1 \sinh a) \end{aligned}$$

$$\begin{aligned} \Lambda_3 &= \Delta_{15} - \Delta_{16} \\ \Delta_{15} &= \frac{(4a^2 E_2 + 6a^2 E_1 + 6E_2)}{24a^3} (a_3 \cosh a + a_2 \sinh a) \\ \Delta_{16} &= \frac{(E_2 + E_1)}{4a^2} (a_3 \sinh a + a_2 \cosh a) \end{aligned}$$

4.2. Parabolic temperature profile.

For the parabolic temperature profile

$$h(z) = 2z \quad \text{and} \quad h_m(z_m) = 2z_m \tag{30}$$

Substituting (30) into (20) and (22), the temperature distributions $\theta(z)$ and $\theta_m(z_m)$ are obtained using the temperature boundary conditions is as follows

$$\theta(z) = A_1 [c_5 \cosh az + c_6 \sinh az + g_2(z)] \tag{31}$$

$$\theta_m(z_m) = A_1 [c_7 \cosh a_m z_m + c_8 \sinh a_m z_m + g_{2m}(z_m)] \tag{32}$$

where

$$g_2(z) = A_1 [\Delta_{17} - \Delta_{18} + \Delta_{19} - \Delta_{20}], \quad g_{2m}(z_m) = A_1 [\Delta_{21} - \Delta_{22}]$$

$$\Delta_{17} = \frac{(2E_3 z + E_4 z^2)}{4a} (a_1 \cosh az + \sinh az)$$

$$\Delta_{18} = \frac{E_4 z}{4a^2} (\cosh az + a_1 \sinh az)$$

$$\Delta_{19} = \frac{(6a^2 z^2 E_3 + 4a^2 z^3 E_4 + 6E_4 z)}{24a^3} (a_3 \cosh az + a_2 \sinh az)$$

$$\Delta_{20} = \frac{(E_3 z + E_4 z^2)}{4a^2} (a_2 \cosh az + a_3 \sinh az)$$

$$\Delta_{21} = \frac{(2E_{3m} z_m + E_{4m} z_m^2)}{4a_m} (a_5 \cosh a_m z_m + a_4 \sinh a_m z_m)$$

$$\Delta_{22} = \frac{E_{4m} z_m}{4a_m^2} (a_4 \cosh a_m z_m + a_5 \sinh a_m z_m)$$

$$E_3 = R_I^*, \quad E_4 = -2(R_I^* + 1), \quad E_{3m} = -R_{Im}^*, \quad E_{4m} = -2(R_{Im}^* + 1)$$

$$c_5 = c_7 \hat{T}, \quad c_6 = \frac{1}{a} (c_8 a_m + \delta_{12} - \delta_{11}),$$

$$c_7 = \frac{\delta_{15}}{\delta_{16}}, \quad c_8 = \frac{\delta_{17}}{\delta_{18}}$$

$$\delta_{10} = -A_1 [\Delta_{23} + \Delta_{24} + \Delta_{25} + \Delta_{26}]$$

$$\Delta_{23} = \frac{(2a^2 E_3 + E_4 (a^2 - 1))}{4a^2} (\cosh a + a_1 \sinh a)$$

$$\Delta_{24} = \frac{E_4 + 2E_3}{4a} (a_1 \cosh a + \sinh a)$$

$$\Delta_{25} = \frac{(3a^2 - 3)E_3 + (2a^2 - 3)E_4}{12a^2} (a_2 \cosh a + a_3 \sinh a)$$

$$\Delta_{26} = \frac{(a^2 E_3 + E_4 (a^2 + 1))}{4a^3} (a_3 \cosh a + a_2 \sinh a)$$

$$\delta_{11} = A_1 \left[\frac{(2a^2 a_1 - a a_2) E_3 + (a_3 - a) E_4}{4a^3} \right]$$

$$\begin{aligned} \delta_{12} &= A_1 \left[\frac{2E_{3m}a_5}{4a_m} - \frac{a_4E_{4m}}{4a_m^2} \right] \\ \delta_{13} &= -A_1 [\Delta_{27} + \Delta_{28}] \\ \Delta_{27} &= \left[\frac{E_{4m} - 2E_{3m}}{4a_m} \right] (a_5 \cosh a_m - a_4 \sinh a_m) \\ \Delta_{28} &= \left[\frac{E_{4m}}{4a_m^2} \right] (a_4 \cosh a_m - a_5 \sinh a_m) \\ \delta_{14} &= \delta_{10} - (\delta_{12} - \delta_{11}) \cosh a, \delta_{15} = \delta_{13}a_m \cosh a + \delta_{14} \sinh a_m \\ \delta_{16} &= a_m \cosh a_m \cosh a + a\widehat{T} \sinh a \sinh a_m \\ \delta_{17} &= \delta_{13}a\widehat{T} \sinh a - \delta_{14} \cosh a_m \\ \delta_{18} &= -a \sinh a_m \widehat{T} \sinh a - a_m \cosh a \cosh a_m \end{aligned}$$

From the boundary condition (23)¹, the thermal Marangoni number for parabolic temperature profile is as follows

$$M_2 = \frac{-\Lambda_1}{a^2(c_5 \cosh a + c_6 \sinh a + \Lambda_4 + \Lambda_5)} \tag{33}$$

where

$$\begin{aligned} \Lambda_4 &= \left(\frac{E_4 + 2E_3}{4a} \right) (a_1 \cosh a + \sinh a) - \frac{E_4}{4a^2} (\cosh a + a_1 \sinh a) \\ \Lambda_5 &= \Delta_{29} - \Delta_{30} \\ \Delta_{29} &= \frac{(4a^2E_4 + 6a^2E_3 + 6E_4)}{24a^3} (a_3 \cosh a + a_2 \sinh a) \\ \Delta_{30} &= \frac{(E_4 + E_3)}{4a^2} (a_3 \sinh a + a_2 \cosh a) \end{aligned}$$

4.3. *Inverted Parabolic temperature profile.*

Consider this profile

$$h(z) = 2(1 - z) \quad \text{and} \quad h_m(z_m) = 2(1 - z_m) \tag{34}$$

Substituting (34) into (20) and (22), the temperature distributions $\theta(z)$ and $\theta_m(z_m)$ are obtained using the temperature boundary conditions, as follows

$$\theta(z) = A_1 [c_9 \cosh az + c_{10} \sinh az + g_3(z)] \tag{35}$$

$$\theta_m(z_m) = A_1 [c_{11} \cosh a_m z_m + c_{12} \sinh a_m z_m + g_{3m}(z_m)] \tag{36}$$

where

$$\begin{aligned} g_3(z) &= A_1 [\Delta_{31} - \Delta_{32} + \Delta_{33} - \Delta_{34}], g_{3m}(z_m) = A_1 [\Delta_{35} - \Delta_{36}] \\ \Delta_{31} &= \frac{(2E_5z + E_6z^2)}{4a} (a_1 \cosh az + \sinh az) \\ \Delta_{32} &= \frac{E_6z}{4a^2} (\cosh az + a_1 \sinh az) \\ \Delta_{33} &= \frac{(6a^2z^2E_5 + 4a^2z^3E_6 + 6E_6z)}{24a^3} (a_3 \cosh az + a_2 \sinh az) \\ \Delta_{34} &= \frac{(E_5z + E_6z^2)}{4a^2} (a_2 \cosh az + a_3 \sinh az) \\ \Delta_{35} &= \frac{(2E_{5m}z_m + E_{6m}z_m^2)}{4a_m} (a_5 \cosh a_m z_m + a_4 \sinh a_m z_m) \end{aligned}$$

$$\begin{aligned} \Delta_{36} &= \frac{E_{6m}z_m}{4a_m^2}(a_4 \cosh a_m z_m + a_5 \sinh a_m z_m) \\ E_5 &= R_I^* - 2, E_6 = 2(1 - R_I^*), E_{5m} = -2 - R_{Im}^*, E_{6m} = 2(1 - R_{Im}^*) \\ c_9 &= c_{11}\hat{T}, c_{10} = \frac{1}{a}(c_{12}a_m + \delta_{22} - \delta_{21}), \\ c_{11} &= \frac{\delta_{24}}{\delta_{25}}, c_{12} = \frac{\delta_{26}}{\delta_{27}} \\ \delta_{19} &= -A_1[\Delta_{37} + \Delta_{38} + \Delta_{39} + \Delta_{40}] \\ \Delta_{37} &= \frac{(2a^2 E_5 + E_6(a^2 - 1))}{4a^2}(\cosh a + a_1 \sinh a) \\ \Delta_{38} &= \frac{E_6 + 2E_5}{4a}(a_1 \cosh a + \sinh a) \\ \Delta_{39} &= \frac{(3a^2 - 3)E_5 + (2a^2 - 3)E_6}{12a^2}(a_2 \cosh a + a_3 \sinh a) \\ \Delta_{40} &= \frac{(a^2 E_5 + E_6(a^2 + 1))}{4a^3}(a_3 \cosh a + a_2 \sinh a) \\ \delta_{20} &= -A_1[\Delta_{41} + \Delta_{42}] \\ \Delta_{41} &= \left[\frac{E_{6m} - 2E_{5m}}{4a_m}\right](a_5 \cosh a_m - a_4 \sinh a_m) \\ \Delta_{42} &= \left[\frac{E_{6m}}{4a_m^2}\right](a_4 \cosh a_m - a_5 \sinh a_m) \\ \delta_{21} &= A_1\left[\frac{(2a^2 a_1 - aa_2)E_5 + (a_3 - a)E_6}{4a^3}\right] \\ \delta_{22} &= A_1\left[\frac{2E_{5m}a_5}{4a_m} - \frac{a_4 E_{6m}}{4a_m^2}\right] \\ \delta_{23} &= \delta_{19} - (\delta_{22} - \delta_{21}) \cosh a, \delta_{24} = \delta_{22}a_m \cosh a + \delta_{23} \sinh a_m \\ \delta_{25} &= a_m \cosh a_m \cosh a + a\hat{T} \sinh a \sinh a_m \\ \delta_{26} &= \delta_{22}a\hat{T} \sinh a - \delta_{23} \cosh a_m \\ \delta_{27} &= -a \sinh a_m \hat{T} \sinh a - a_m \cosh a \cosh a_m \end{aligned}$$

From the boundary condition (23)¹, the thermal Marangoni number for inverted parabolic temperature profile is as follows

$$M_3 = -\frac{\Lambda_1}{a^2(c_9 \cosh a + c_{10} \sinh a + \Lambda_6 + \Lambda_7)} \tag{37}$$

where

$$\begin{aligned} \Lambda_6 &= \left(\frac{E_6 + 2E_5}{4a}\right)(a_1 \cosh a + \sinh a) - \frac{E_6}{4a^2}(\cosh a + a_1 \sinh a) \\ \Lambda_7 &= \Delta_{43} - \Delta_{44} \\ \Delta_{43} &= \frac{(4a^2 E_6 + 6a^2 E_5 + 6E_6)}{24a^3}(a_3 \cosh a + a_2 \sinh a) \\ \Delta_{44} &= \frac{(E_6 + E_5)}{4a^2}(a_3 \sinh a + a_2 \cosh a). \end{aligned}$$

5. RESULTS AND DISCUSSION

The stability analysis of Bènard-Marangoni convection in a composite layer with fluid saturated porous layer beneath the fluid layer in the presence of heat source (sink) with non-uniform temperature gradients is studied theoretically. The Eigen value problem thus obtained has an exact solution. Thermal Marangoni number M is the Eigen value of the system. The strength of the heat source (sink) considered, represented by internal Rayleigh number R_I is small so that the convection is not induced by itself. The variation of these on the thermal Marangoni number are represented graphically in the following figures for all the three temperature profiles for fixed values of $a = R_I = R_{Im} = \hat{T} = 1$ and $\beta = 0.1$.

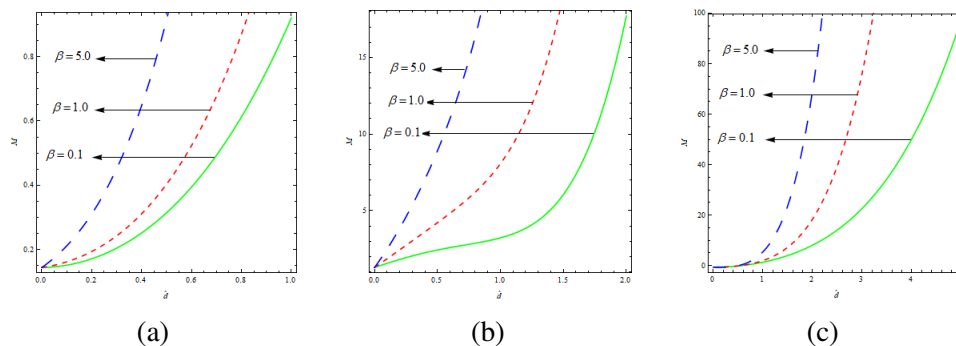


FIGURE 1. Effects of porous parameter β

The effect of porous parameter β , on thermal Marangoni number is recorded in the figures 1a, 1b and 1c for the three different temperature profiles. From the figures it can be noted that the effect of β , for a given depth ratio \hat{d} , is to increase M irrespective of the temperature profiles. It can be clearly observed that $M_1(\hat{d}) < M_2(\hat{d}) < M_3(\hat{d})$ there by indicating that the increase in depth ratio is to stabilize the system. Also one can conclude, from figure 1c that the increase in depth ratio beyond one (indicating that the porous layer dominant composite layer) increases M more rapidly. The diverging nature of the curves indicate that the effect is drastic for larger depth ratio. This implies that the inverted parabolic temperature profile brings in greater stability for porous layer dominant composite layers.

Figures 2a, 2b, 2c are the plots of M versus \hat{d} for different internal Rayleigh number R_I , in the fluid region. From Fig. 2a it is observed that the effect of R_I is to destabilize the system and the effect of increasing \hat{d} (0 to 1) is to stabilize the system in the case of linear temperature profile. The reverse is observed for increasing \hat{d} in the case of parabolic temperature profile, up to a certain value and then M increases for the porous layer dominant composite layer. The results for R_I are qualitatively similar for all the temperature profiles. It can also be seen from these figures that the effect of R_I for inverted parabolic temperature profile is not much as compared to the other two profiles. From these figures one can also conclude

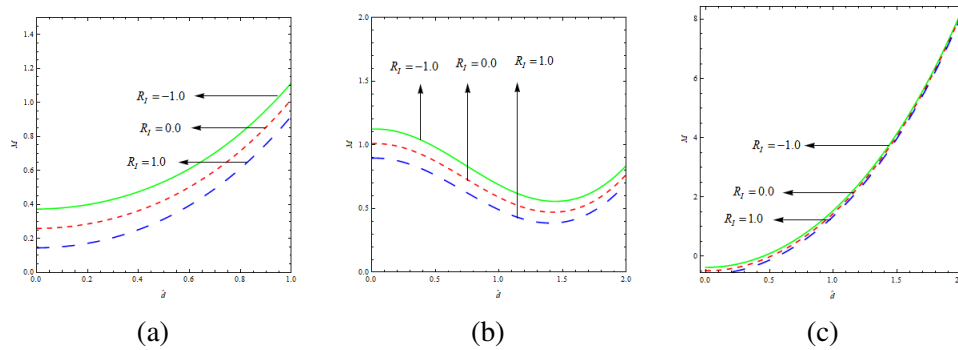


FIGURE 2. Effects of fluid internal Rayleigh number R_I

that $M_1(\widehat{d}) < M_2(\widehat{d}) < M_3(\widehat{d})$. The converging nature of the curves imply that the effect is more in the fluid layer dominant composite layer.

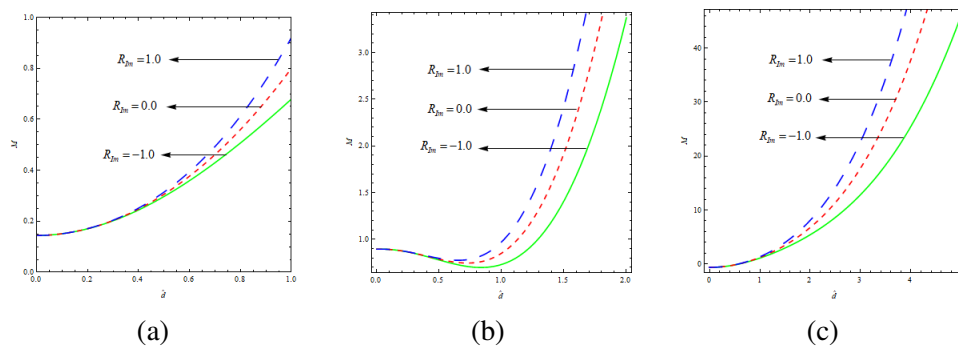
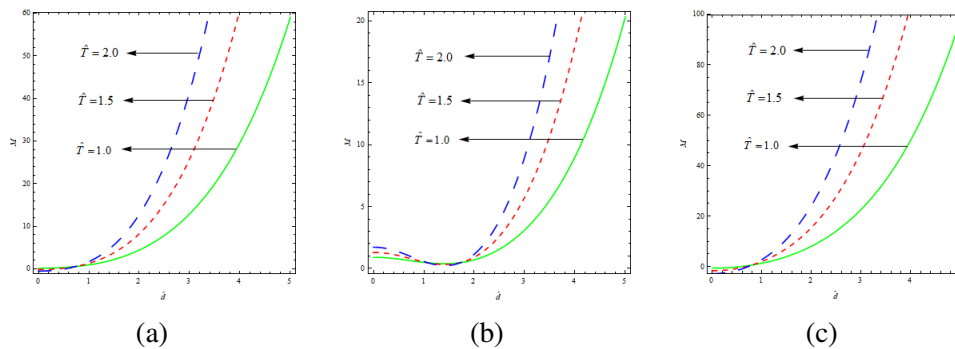


FIGURE 3. Effects of porous internal Rayleigh number R_{Im}

Effect of R_{Im} , internal Rayleigh number in the porous layer on M for three different temperature profiles are depicted in figures 3a, 3b, 3c. The values of R_{Im} are chosen as $-1, 0$ and 1 which represent the presence of sink, no source (sink) and a source. It is observed that for all the temperature profiles, the effect of R_{Im} is to stabilize the system as the values increase from -1 to 1 . It can also be seen that the effect of R_{Im} is clearly visible for a larger \widehat{d} . This implies that the dominance of porous layer causes stability. Marangoni number is quite large for the inverted parabolic temperature profile as compared to the other two temperature profiles. These results are qualitatively opposite to the results for R_I (Figs. 2a, 2b, 2c).

Figures 4a, 4b and 4c are the plots of M versus \widehat{d} for different thermal ratio \widehat{T} , which includes the effect of boundary temperatures along with the interfacial temperature, for all the three temperature profiles. As expected the effect of \widehat{T} is to increase M . The diverging nature of the curves indicate that the effect of \widehat{T} is more pronouncing in the porous layer dominant composite layer.

FIGURE 4. Effects of thermal ratio \hat{T}

6. CONCLUSION

Following conclusions are drawn from this study

- (i) $M_1(\hat{d}) < M_2(\hat{d}) < M_3(\hat{d})$
- (ii) Depth ratio, internal Rayleigh number, porous parameter and thermal ratio can be effectively used to control the convection.
- (iii) Inverted parabolic temperature profile is the most stable among all the three different temperature profiles considered.

REFERENCES

- [1] Nield, D. A., *Onset of convection in a fluid layer overlying a layer of porous medium*, J. Fluid Mech., **81** (1977), 513-522.
- [2] McKay, G., *Onset of buoyancy driven convection in a superposed reacting fluid and porous layers*, J. Engg. Math., **33** (1998), 31-46.
- [3] Taslim, M. E. and Narusawa, V., *Thermal stability of horizontally superposed fluid and porous layer*, ASME J. Heat Transf., **111** (1989), 357-362.
- [4] Chen, F., *Through-flow effects on convective instability in superposed fluid and porous layers*, J. Fluid Mech., **231** (1990), 113-133.
- [5] Nield, D. A. and Bejan, A., *Convection in Porous Media*, Third ed. Springer-Verlag, New York, (2006).
- [6] Straughan, B., *Surface tension driven convection in a fluid overlying a porous layer*, Comput. Phys., **170** (2001), 320-337.
- [7] Straughan, B., *Stability and wave motion in porous media*, Appl. Math. Sci. Ser., **165** (2008), Springer, New York.
- [8] Carr, M., *Penetrative convection in a superposed porous medium-fluid layer via internal heating*, J. Fluid Mech., **509** (2004), 305-329.
- [9] Chang, M. H., *Stability of convection induced by selective absorption of radiation in a fluid overlying a porous layer*, Phys. Fluids, **16** (2004), 3690-3698.
- [10] Chang, M. H., *Thermal convection in superposed fluid and porous layers subjected to a horizontal plane Couette flow*, Phys. Fluids, **17** (2005), 064106-064106-7.
- [11] Chang, M. H., *Thermal convection in superposed fluid and porous layers subjected to a plane Poiseuille flow*, Phys. Fluids, **18** (2006), 035104-035104-10.
- [12] Shivakumara, I. S., Suma, S. P. and Chavaraddi, K. B., *Onset of surface tension driven convection in superposed fluid and porous layers*, Arch. Mech., **55** (2006), 327-348.
- [13] Shivakumara, I. S., Lee, J. and Chavaraddi, K. B., *Onset of surface tension convection in a fluid layer overlying a layer of anisotropic porous medium*, Int. J. Heat and Mass Transfer, **54** (2011), 994-1001.

- [14] Shivakumara, I. S., Suma, S. P. Indira, R. and Gangadharaiyah, Y. H. , *Effect of internal heat generation on the onset of Marangoni convection in a fluid layer overlying a layer of anisotropic porous medium*, Trans. Porous Med., **92** (2012), 727-743.
- [15] Liancun Zheng., YanhaiLin and Xinxin Zhang., *Marangoni convection of power law fluids driven by power-law temperature gradient*, Journal of the Franklin Institute, **349** (2012), no. 8, 2585-2597.
- [16] Sumithra R and Manjunatha N., *Analytical study of surface tension driven magneto convection in a composite layer bounded by adiabatic boundaries*, International Journal of Engineering and Innovative Technology, **1** (2012), no.6 , 249-257.
- [17] Sumithra R., *Double diffusive magneto-Marangoni convection in a composite layer*, International Journal of Application or Innovation in Engineering & Management, **3** (2014), no. 2, 12-25.
- [18] Tatiana Gambaryam-Roisman., *Historical prespective modulation of Marangoni convection in liquid films*, Advances in Colloid and Interface Science, **222** (2015), 319-331.
- [19] Yaofa Li and Minami Yoda., *An experimental study of buoyancy-Marangoni convection in confined and volatile binary fluids*, International Journal of Heat and Mass Transfer, **102** (2016), 369-380.
- [20] Sankaran. A. and Yarin, A.L., *Evaporation-driven thermocapillary Marangoni convection in liquid layers of different depths*, International Journal of Heat and Mass Transfer, **122** (2018), 504-514.
- [21] Ananda, K. and Gangadharaiyah, Y.H., *Influence of vertical magnetic field on the onset of Rayleigh-Benard-Marangoni convection in superposed fluid and porous layers with deformable free surface*, International Journal of Scientific Research in Mathematical and Statistical Sciences, **5** (2018), no. 5, 1-18.
- [22] Manjunatha N and Sumithra R., *Effects of non-uniform temperature gradients on double diffusive Marangoni convection in a two layer system*, International Journal pure and applied mathematics, **118** (2018), no.2, 203-219.
- [23] Vanishree R.K., *Effects of Through-flow and internal heat generation on a thermo convective instability in an anisotropic porous medium*, Journal of Applied Fluid Mechnaics, **7** (2014), no.4, 581-590.
- [24] Siddheshwar P.G. and Vanishree R.K., *Lorenz and Ginzburg-Landau equations for thermal convection in a high-porosity medium with heat source*, Ain Shams J. Engg., **9** (2018), 1547-1555.